BIOCHEMISTRY
including biophysical chemistry & molecular biology
Article

Biochemistry **2010,** *49,* 2433–2442 2433
DOI: 10.1021/bi9022285

Constitutive NADPH-Dependent Electron Transferase Activity of the Nox4 Dehydrogenase Domain†

Yukio Nisimoto,‡,∥ Heather M. Jackson,‡,∥ Hisamitsu Ogawa,§ Tsukasa Kawahara,‡ and J. David Lambeth*,‡

‡*Department of Pathology and Laboratory Medicine, Emory University Medical School, Atlanta, Georgia 30322, and* §*Department of Biology, Fujita Health University, School of Medicine, Toyoake, Aichi 470-1192, Japan*
∥*These authors contributed equally to this work.*

Received December 31, 2009; Revised Manuscript Received February 16, 2010

ABSTRACT: NADPH oxidase 4 (Nox4) is constitutively active, while Nox2 requires the cytosolic regulatory subunits $p47^{phox}$ and $p67^{phox}$ and activated Rac with activation by phorbol 12-myristate 13-acetate (PMA). This study was undertaken to identify the domain on Nox4 that confers constitutive activity. Lysates from Nox4-expressing cells exhibited constitutive NADPH- but not NADH-dependent hydrogen peroxide production with a K_m for NADPH of 55 ± 10 μM. The concentration of Nox4 in cell lysates was estimated using Western blotting and allowed calculation of a turnover of ~200 mol of H_2O_2 min^{-1} (mol of Nox4)$^{-1}$. A chimeric protein (Nox2/4) consisting of the Nox2 transmembrane (TM) domain and the Nox4 dehydrogenase (DH) domain showed H_2O_2 production in the absence of cytosolic regulatory subunits. In contrast, chimera Nox4/2, consisting of the Nox4 TM and Nox2 DH domains, exhibited PMA-dependent activation that required coexpression of regulatory subunits. Nox DH domains from several Nox isoforms were purified and evaluated for their electron transferase activities. Nox1 DH, Nox2 DH, and Nox5 DH domains exhibited barely detectable activities toward artificial electron acceptors, while the Nox4 DH domain exhibited significant rates of reduction of cytochrome *c* (160 min^{-1}, largely superoxide dismutase-independent), ferricyanide (470 min^{-1}), and other electron acceptors (artificial dyes and cytochrome b_5). Rates were similar to those observed for H_2O_2 production by the Nox4 holoenzyme in cell lysates. The activity required added FAD and was seen with NADPH but not NADH. These results indicate that the Nox4 DH domain exists in an intrinsically activated state and that electron transfer from NADPH to FAD is likely to be rate-limiting in the NADPH-dependent reduction of oxygen by holo-Nox4.

Reactive oxygen species (ROS),[1] which include superoxide anion and its metabolites, are critically important both in phagocytic cells where they participate in killing bacteria and in other cell types where they function as signaling molecules. A major source of these biologically generated molecular species is the reactive oxygen-generating NADPH oxidases or Nox enzymes. The activation mechanisms of these enzymes differ among the seven Nox isoforms (Nox1−5, Duox1, and Duox2) expressed in human tissue. The phagocyte Nox, also known as the respiratory burst oxidase, has been extensively studied. The enzyme generates high levels of ROS in activated neutrophils and macrophages and functions as a defense enzyme to kill invading microbes. The oxidase consists of a membrane-associated catalytic subunit Nox2 (also known as $gp91^{phox}$) that forms a heterodimer with the small membrane subunit, $p22^{phox}$. Activation involves the assembly of the membrane-bound heterodimer with cytosolic regulatory subunits $p47^{phox}$, $p67^{phox}$, and $p40^{phox}$ and the GTP-bound form of the small GTPase Rac (Rac1 or Rac2). The Nox2 catalytic subunit consists of two domains, a cytosol-facing dehydrogenase (DH) domain that contains a binding site for NADPH and one for FAD (*1*−*3*) and a membrane domain consisting of six transmembrane (TM) helices that bind two heme groups (hemes A and B) localized approximately at the levels of the two leaflets of the membrane bilayer. In the activated enzyme, electrons pass from NADPH to the FAD and then through both heme groups to reduce molecular oxygen to form the superoxide transmembrane to the cytosol (i.e., either in the phagosome or outside the cell). Evidence points to the DH domain of Nox2 as the target of regulation by activator subunits (*4*, *5*) and indicates that the transfer of a hydride from NADPH to FAD is the rate-determining step that is regulated by the "activation domain" on $p67^{phox}$ (*6*).

Regulated ROS production at considerably lower levels than in neutrophils has been seen in a variety of nonphagocytic cells, where it plays an important role in a range of physiological processes. NADPH oxidase 1 (Nox1) is closely related to Nox2 (~60% amino acid sequence identity) (*7*) and is expressed most strongly in the gastrointestinal tract (*8*, *9*) and in vascular smooth muscle exposed to angiotensin II (*10*, *11*). Like Nox2, Nox1 activity is regulated by Rac, along with two regulatory subunits, NOXO1 and NOXA1 (*12*−*15*), homologues of $p47^{phox}$ and $p67^{phox}$,

†This work was supported by National Institutes of Health Grant CA105116 and American Heart Association Grant 0815088E.

*To whom correspondence should be addressed: Department of Pathology and Laboratory Medicine, Emory University Medical School, Atlanta, GA 30322. Phone: (404) 727-5875. Fax: (404) 727-8538. E-mail: noxdoc@mac.com.

[1]Abbreviations: TM, transmembrane; DH, dehydrogenase; ROS, reactive oxygen species; O_2^-, superoxide anion; SOD, superoxide dismutase; HRP, horseradish peroxidase; *phox*, phagocyte oxidase; PMA, phorbol 12-myristate 13-acetate; IPTG, isopropyl β-D-thiogalactoside; MBP, maltose-binding protein; PMSF, phenylmethanesulfonyl fluoride; DPI, diphenyleneiodonium; PCR, polymerase chain reaction.

Published on Web 02/17/2010

respectively. Nox3 is expressed in the inner ear (*16*) and is activated by NOXO1 (*17*−*19*). Nox4 is widely expressed, with its strongest expression in the kidney (*20*, *21*). While Nox1−3 comprise a close, evolutionarily related subgroup, Nox4 is more distantly related, with ~39% amino acid identity with Nox2 (*21*). Like the Nox1−3 subfamily, Nox4 requires $p22^{phox}$ for activity, but unlike Nox1−3, Nox4 does not require the proline-rich sequence in $p22^{phox}$ that is the target of regulatory subunit binding (*22*), consistent with its lack of a requirement for regulatory subunits other than $p22^{phox}$ (*23*, *24*). Indeed, Nox4 is unique among the Nox enzymes in that it is constitutively active (*20*, *25*). In addition to the $p22^{phox}$-requiring Noxes, mammals express the calcium-activated Nox enzymes Nox5, Duox1, and Duox2, all of which possess an EF-hand-contining Ca^{2+}-binding domain (*26*−*28*).

Because expressed Nox4 does not require any known activators, regulatory subunits, or regulatory domains, we compared the properties of Nox4 with those of other Nox homologues that might account for its constitutive activity. Previous studies of Nox2 pointed to the transfer of hydride from NADPH to FAD, which occurs within the DH domain, as the rate-determining and subunit-regulated step (*4*, *5*). However, other studies suggested that FAD-to-heme electron transfer may also be regulated in Nox2 (*29*). Herein, we investigated the hypothesis that the constitutive activity of Nox4 resides in its DH domain. This domain, located immediately C-terminal to the TM domain, is homologous to a number of soluble dehydrogenase-type flavoproteins (*1*−*3*) and is therefore predicted to form an independently folding DH domain that is localized at the cytosolic side of the membrane. We find that the DH domain of Nox4 is constitutively "turned on" compared with the DH domains of Nox1−3, and this property of the DH domain accounts for the constitutive activity of the holoenzyme.

MATERIALS AND METHODS

Materials. Full-length cDNA encoding human Nox4 (amino acid residues 1−578) and cDNA of chimeric Noxes, Nox2/4 (residues 1−284 of Nox2 fused to residues 298−578 of Nox4), and chimera Nox4/2 (residues 1−337 of Nox4 connected to residues 324−570 of Nox2) were cloned into pcDNA3 (Invitrogen). cDNA encoding Nox DH domains (Nox1, -2, -4, and -5) were subcloned into pMAL-C2X (New England Biolabs). DH domains corresponded to residues 283−570 for Nox1, 283−570 for Nox2, 304−578 for Nox4, and 405−737 for Nox5. These constructs, producing MBP-tagged C-terminal Nox homologues, were expressed in *Escherichia coli* BL-21. The goat anti-rabbit IgG secondary antibody linked to horseradish peroxidase and prestained molecular weight markers for SDS−PAGE were from Bio-Rad. The polyclonal antibody to a C-terminal peptide (residues 500−578) of Nox4 was from Novus Biologicals Inc., and the monoclonal antibody to MBP, amylose agarose, and Factor Xa protease were from New England Biolabs. Protease inhibitor cocktail was from Roche, and ferricytochrome *c*, nitroblue tetrazolium (NBT), *p*-iodonitrotetrazolium violet (INT), dichloroindophenol (DCIP), potassium ferricyanide, FAD, NADPH, NADH, maltose, diphenyleneiodonium (DPI), and protein A-agarose Fast flow [50% (v/v)] were purchased from Sigma Aldrich (St. Louis, MO).

Generation of cDNA Encoding a Nox2/4 Chimera. Chimera Nox2/4 consists of the TM domain of Nox2 (residues 1−284) and the Nox4 DH domain (residues 298−578). Chimera Nox4/2 consists of the Nox4 TM domain (residues 1−337) and the Nox2 DH domain (residues 324−570). Chimeric constructs were created by two consecutive PCRs. The following primers were used to create Nox4/2: (1) human Nox4 sense primer with the BamHI site underlined and with a kozak sequence, 5′-ttttggatccgccaccatggctgtgtcctggaggagctggctcgccaacga-3′; (2) Nox4/2 sense primer with the Nox2 sequence underlined, 5′-tttaaagcaagacctggtcagtacatttttgtcaagtgccca-3′; (3) Nox4/2 antisense primer with the Nox2 sequence underlined (reverse complement of primer 2), 5′-tgggcacttgacaaaaatgtactgaccaggtcttgctttaaa-3′; (4) Nox2 antisense primer from the end of the sequence with the NotI site underlined, 5′-ttttgcggccgcttagaagttttccttgttgaaaatgaaatgcac-3′. The following primers were used to create chimera Nox2/4: (5) human Nox2 sense primer with the BamHI site underlined and with a kozak sequence, 5′-ttttggatccaccAtggggaactgggctgtgaatgaggggctc-3′; (6) Nox2/4 sense primer with the Nox2 sequence underlined, 5′-ccatgtttctgtatctctgtgaaagactttacaggtatatccggagcaa-3′; (7) Nox2/4 antisense primer with the Nox2 sequence underlined, 5′-ttgctccggatatacctgtaaagtctttcacagagatacagaaacatgg-3′; (8) Nox4 antisense sequence with the NotI site underlined, 5′-ttttgcggccgcctagctgaaagactctttattgtattc-3′. PCR A used primers 1 and 3 to amplify human Nox4 TM domain cDNA, primers 5 and 7 to amplify human Nox2 TM domain cDNA, primers 2 and 4 to amplify Nox2 DH domain cDNA, and primers 6 and 8 to amplify Nox4 DH domain cDNA. PCR B used primers 1 and 4 to amplify PCR A products of Nox4 TM and Nox2 DH domains and primers 5 and 8 to amplify PCR A products of Nox2 TM and Nox4 DH domains. PCR products from reaction B were digested with BamHI and NotI and ligated into the mammalian expression vector, pcDNA3 (Invitrogen). Sequences were confirmed by commercial DNA sequencing (Agencourt Biosciences Corp.).

Transfection. HEK293 cells were cultured in Dulbecco's modified Eagle's medium (Gibco) containing 4.6 mg/mL glucose, 4.6 mg/mL L-glutamate, 10% fetal serum (Atlanta Biologicals), 100 units/mL penicillin, and 0.1 mg/mL streptomycin (Gibco) in 5% CO_2 at 37 °C for 24 h. Cells were transfected with cDNA encoding human full-length Nox4, full-length Nox2, the Nox2/4 chimera, the Nox4/2 chimera in vector pcDNA3, or empty pcDNA3 with and without co-expression of regulatory subunits (human Rac1G12 V, $p47^{phox}$, and $p67^{phox}$), using the FuGene 6 (Roche Molecular Biochemicals) transfection system according to the manufacturer's instructions. After 48 h, cells were harvested and washed twice with Hank's balanced salt solution (HBSS). The cells pelleted at 2000*g* for 5 min were suspended in HBSS for the NADPH oxidase assay of intact cells and in breaking buffer for the cell-free oxidase assay.

Hydrogen Peroxide Generating Activity. Pyridine nucleotide-dependent H_2O_2 producing activity was examined in intact HEK293 cells and the cell lysates. Cells (~2×10^7) in 2 mL of ice-cold disruption buffer (PBS containing 0.1 mM EDTA, 10% glycerol, 0.2 mM FAD, 1 μg/mL protease inhibitor cocktail, and 0.1 mM PMSF) were disrupted by sonication (2×10 s) in a bath sonicator at 3 °C, according to the previously described methods (*30*). ROS generation was assessed by either Luminol chemiluminescence increase using a FluoStar luminometer (BMG Labtech) or the fluorescence increase at 620 nm with a bandwidth of 40 nm (excitation wavelength of 540 nm with a bandwidth of 25 nm) due to H_2O_2-dependent Amplex Red oxidation in the presence of HRP using a Synergy 2 Multi-Mode Microplate Reader and Gen5 (Bio Tek). A standard curve of known H_2O_2 concentrations was developed using the Amplex Red assay and was used to quantify H_2O_2 concentration. In the whole cell assay,

$5-7 \times 10^4$ cells were added to 0.1 mL of assay buffer [25 mM Hepes (pH 7.4) containing 0.12 M NaCl, 3 mM KCl, 1 mM $MgCl_2$, 0.1 mM Amplex Red, and 0.032 unit of HRP]. In the cell-free assay, the reaction was started via addition of an appropriate amount (30−50 μg of protein) of the cell lysates to 0.1 mL of the assay mixture (assay buffer containing 25 μM FAD and 36 μM NADPH or 36 μM NADH). The reaction was monitored at 25 °C for 10 min, and the emission increase was linear during this interval. Reaction rates determined in the cell lysates were normalized to 10^7 cells on the basis of the total protein equivalents, 4.53 mg/10^7 cells for vector-transfected cell lysates and 4.16 mg/10^7 cells for Nox4-transfected cell lysates.

Spectrophotometric Measurements of Heme in Cell Extracts of HEK293. Whole cell extracts were prepared using the Nonidet P-40 lysis buffer according to a previously described method (*31*). Cells were incubated for 30 min in ice-cold Nonidet P-40 lysis buffer [50 mM Tris-HCl (pH 7.5), 0.12 M NaCl, 5 mM EDTA, 5 mM EGTA, 1% Nonidet P-40, and 5% glycerol]. Lysates were centrifuged at 14000*g* for 20 min, and the supernatant was collected. The extracts of HEK293 cells transfected with vector alone or vector encoding Nox4 were used for the quantification of heme. Reduced spectra were recorded at 10 min intervals after addition of a few crystals of sodium dithionite until a stable spectrum was achieved. A molar absorption coefficient (ε_{414}) of 130 mM^{-1} cm^{-1} (*32*) for the Soret band was used for calculations.

Expression of Nox1, Nox2, Nox4, and Nox5 DH Domains. A series of truncated Nox clones was obtained by PCR using each Nox cDNA cloned in the pMAL-C2X plasmid as the template. According to previously described methods (*4*), PCR products for truncated Nox1 DH (residues 283−570), Nox2 DH (residues 283−570), Nox4 DH (residues 304−578), and Nox5 DH (residues 405−737) domains were purified using a PCR purification kit (Qiagen). The purified DNA fragments were ligated into the EcoRI and SalI sites for the Nox1 DH domain, BamHI and HindIII for the Nox2 DH domain, and BamHI and SalI for Nox4 DH and Nox5 DH domains in pMAL-C2X vector and transformed into *E. coli*. Transformants were selected from LB/ampicillin plates, and plasmids were isolated from 2 mL cultures of transformants as described previously (*4*). The plasmids were digested with restriction enzymes and were separated on 1% agarose to confirm the presence of the insert. DNA sequences of all clones were confirmed by nucleotide sequencing.

Expression and Purification of Nox DH Proteins. MBP fusion proteins were induced in *E. coli* at 37 °C by addition of 0.1 mM IPTG for 2.5 h and frozen at −80 °C. Thawed cells were sonicated (3 × 15 s) and solubilized in 50 mM Hepes buffer (pH 7.5) containing 0.5 M NaCl, 1 mM PMSF, 1 mM EDTA, 1 mM dithiothreitol, protease inhibitor cocktail (1 μg/mL), and 0.2 M L-arginine at 3 °C. Arginine was included to improve the yield and minimize protein aggregation (*33*). Purification was conducted by amylose-agarose column chromatography (10 mm × 15 mm) according to instructions from BioLabs, and the fusion proteins were stored at −80 °C in 50 mM Hepes buffer (pH 7.5) containing 0.1 M NaCl, 0.2 M arginine, 1 mM EDTA, 0.2% Tween 20, protease inhibitor cocktail, and 0.1 mM PMSF. Long-term storage was avoided due to gradual proteolysis and loss of activity.

Superoxide Generating Activity. Superoxide generation was assessed using SOD-inhibitable ferricytochrome *c* reduction quantified at 550 nm using an extinction coefficient of 21.1 mM^{-1} cm^{-1} (*34*). The indicated amount of HEK293 cell lysate or isolated Nox DH domain protein was added to 1 mL of assay buffer [25 mM Hepes (pH 7.3) containing 0.25 mM FAD, 0.1 mM ferricytochrome *c*, 0.1 M NaCl, 3 mM KCl, 1 mM $MgCl_2$, and 0.1 mM PMSF], after which 0.2 mM NADPH or 0.2 mM NADH was added, and cytochrome *c* reduction was monitored in the presence and absence of 100 units of SOD at 36 °C.

Pyridine Nucleotide-Dependent Electron Transferring Activity. NADPH-dependent cytochrome *c*, cytochrome b_5, ferricyanide [$K_3Fe(CN)_6$], DCIP, INT, and NBT reductase activities were assayed at 36 °C according to previously described methods (*4*). The activities were assayed in a 1 mL volume of assay buffer [25 mM Hepes buffer (pH 7.3) containing 0.12 M NaCl, 3 mM KCl, 1 mM $MgCl_2$, 0.25 mM FAD, and 80 μM electron acceptor]. After the mixture that included the DH domain had been preincubated for 1 min, the reaction was initiated by the addition of 0.25 mM NADPH or 0.25 mM NADH. A longer preincubation did not affect activity. The reduction rates of electron acceptors were quantified by monitoring the absorbance changes at the appropriate wavelengths, and millimolar extinction coefficients of 21.1 mM^{-1} cm^{-1} at 550 nm (cytochrome *c*) (*34*), 19 mM^{-1} cm^{-1} at 556 nm (cytochrome b_5) (*35*), 1.02 mM^{-1} cm^{-1} at 420 nm (ferricyanide) (*36*), 20 mM^{-1} cm^{-1} at 600 nm (DCIP) (*37*), 10.5 mM^{-1} cm^{-1} at 490 nm (INT) (*38*), and 12.6 mM^{-1} cm^{-1} at 595 nm (NBT) (*39*) were used to calculate the quantity of each electron acceptor reduced. Spectrophotometric measurements were taken using using a Hitachi spectrophotometer with a temperature-controlled cuvette compartment.

Immunoprecipitation and Western Blot Analysis. Nox4 protein was immunoprecipitated from lysates of HEK293 cells and detected by Western blotting. Whole cell extracts were prepared using the Nonidet P-40 lysis buffer as described above. Cell lysates (0.85 mg) from vector alone or Nox4-transfected cells were first precleared with 10 μL of protein A-agarose Fast Flow beads (50% slurry) for 1 h. The supernatant was incubated with 20 μg of antibody to Nox4 and 20 μL of protein A-agarose beads overnight with gentle shaking at 4 °C. The beads were washed three times with lysis buffer, and bound proteins were eluted from the beads into 50 μL of Laemmli sample buffer (Bio-Rad). After SDS−PAGE and after immunoprecipitated proteins had been transferred to an Immobilon PVDF membrane (Millipore), Nox4 was visualized using the same antibody with a horseradish peroxidase-linked secondary antibody (IgG, 1:3000 dilution). Proteins were visualized by chemiluminescence (SuperSignal West Pico Chemiluminescence Substrate, Pierce) or using 3,3′-diaminobenzidine stain (Dojindo). Quantification of immunoprecipitated Nox4 was performed using a standard curve produced with the purified MBP-bound Nox4 DH domain. The integral optical density (IOD) of the Western blot band was estimated using ImageJ.

RESULTS

Pyridine Nucleotide Specificity and Properties of Nox4 Expressed in a Broken Cell Preparation. The Nox2 cell-free system from neutrophil or macrophage cell fractions has been invaluable for the characterization of the enzymatic properties and regulation of the Nox2 system. Lacking an adequate cell that expresses high levels of endogenous Nox4, we used Nox4-transfected versus vector-transfected control cells to characterize Nox4 properties. Hydrogen peroxide and superoxide generation were compared in intact cells and cell lysates using the Amplex Red/HRP assay and cytochrome *c* reduction, respectively. As shown

Table 1: Hydrogen Peroxide Generating Activity (picomoles per minute per 10^7 cells) of HEK293 Cells Expressing Nox4[a]

intact cell assay	control (a)	Nox4 (b)	b − a (%)
HEK293 cells	10.2 ± 2.5	225.9 ± 30.0	215.7 (100)
with DPI	0.85 ± 0.2	4.84 ± 1.0	4.00 (1.9)

	NADPH			NADH		
cell-free assay	control (a)	Nox4 (b)	b − a (%)	control (a)	Nox4 (b)	b − a (%)
cell lysate	74.0 ± 6.3	223.5 ± 18.5	149.5 (69.3)	117.0 ± 25.1	141.4 ± 12.2	24.4 (13)
with DPI	49.2 ± 5.6	101.3 ± 15.2	52.1 (24.2)	78.5 ± 10.3	91.3 ± 7.8	12.8 (5.9)

[a]In the intact cell assay, the reaction was initiated by addition of 5 μL of cells ($5-7 \times 10^4$) to 95 μL of assay buffer (pH 7.5) containing 25 mM Hepes, 120 mM NaCl, 3 mM KCl, 1 mM $MgCl_2$, 0.032 unit of HRP, and 0.1 mM Amplex Red. The fluorescence of Amplex Red was measured for 10 min at 25 °C. In the cell-free oxidase assay, NADPH- or NADH-dependent H_2O_2 generation by cell lysates was monitored in 0.1 mL of the same buffer containing 25 μM FAD and 36 μM NADPH or 36 μM NADH. We initiated the reaction by mixing 30−50 μg of the sample/5 μL of lysate with 95 μL of the assay buffer in the presence or absence of 20 μM DPI. As a control, 5 μL of the cell lysis buffer was added to 95 μL of the reaction mixture instead of the cell lysates. The difference between the fluorescence in the presence and absence of the sample was measured, and the activity (picomoles of H_2O_2 produced per minute per 10^7 cells or milligrams) was calculated using a linear standard curve of the fluorescence intensity vs H_2O_2 concentration (nanomolar). The cell lysates from 10^7 cells transfected with vector alone (control) or Nox4 contained 4.53 ± 0.35 or 4.16 ± 0.30 mg of protein, respectively. Values represent the means ± the standard deviation of three experiments.

in Table 1, intact Nox4-expressing HEK293 cells showed >20-fold higher H_2O_2 generating activity than control cells, and 98% of the Nox4-dependent activity was inhibited with 20 μM DPI. Nearly 70% of the Nox4-dependent activity was retained in the cell lysate when NADPH was used as the electron donor, and the majority of this activity was inhibited with DPI. Minimal Nox4-dependent activity was seen when NADH was used as the electron donor, confirming that the enzyme is specific for NADPH. Consistent with earlier reports (*40*−*42*), H_2O_2 but not superoxide was detectable in Nox4-transfected cells on the basis of the absence of detectable SOD-sensitive cytochrome *c* reduction (data not shown).

As shown in the Lineweaver−Burk plot (Figure 1A), the K_m value of Nox4 for NADPH was determined to be 55 ± 10 μM, a value close to that previously reported for Nox2 (~50 μM) (*43*). Activity required added FAD, but increasing FAD concentrations from 20 to 75 μM did not further stimulate the maximal activity [360 pmol min^{-1} (10^7 cells)$^{-1}$] or change the K_m for NADPH (Figure 1A). Thus, holo-Nox4 is fully saturated at 25 μM FAD added to the cell-free assay system.

Determination of the Turnover Number of Nox4 in Cell Lysates. In cell extracts, we detected a major band of ~75 kDa and a minor band at ~130 kDa by immunoprecipitation and Western blot analysis using an antibody to a C-terminal Nox4 peptide (Figure 1C). A weaker endogenous 75 kDa band was seen in the extracts from control cells (Figure 1B). The Nox4 content in the lysates was estimated using the purified recombinant MBP−Nox4 DH domain fusion protein as a standard (Figure 1D,E) to be 0.38 pmol/mg of extract protein, corresponding to approximately 1.6 pmol of Nox4 per 10^7 cells. This represents only ~5% of the level of Nox2 that is constitutively expressed in neutrophils (~35 pmol/10^7 cells) (*44*−*46*). Assuming most of the Nox4 was immunoprecipitated and neglecting the contribution of the minor 140 kDa band, we found the estimated turnover of Nox4 to be 230 min^{-1}. Spectrophotometric analysis (data not shown) showed an increased heme content of 0.9 pmol/mg in Nox4-transfected compared with control cells. Using this estimate, a similar turnover number was calculated.

ROS Generation by Nox2, Nox4, and Nox2/4 and Nox4/2 Chimeric Proteins in HEK293 Cells. Nox2 activation is dependent on the assembly of cytosolic regulatory subunits, $p67^{phox}$, $p47^{phox}$, and the GTP-bound form of Rac, while Nox4 activity requires none of these additional proteins (*20*, *47*, *48*). To determine whether it is the TM domain or the DH domain that is responsible for conferring the cytosolic subunit-dependent versus constitutive activity, we created chimeric proteins by switching the TM and DH domains of Nox2 and Nox4 as shown in Figure 2A. The cDNA encoding wild-type or chimeric proteins was expressed either without or with $p67^{phox}$, $p47^{phox}$, and Rac1G12V in HEK293 cells, and the resulting ROS generating activities were measured (Figure 2B). As in previous studies (*20*, *25*), wild-type Nox4 exhibited constitutive activity that was unaffected by subunits, while Nox2 activity required coexpression of regulatory subunits. Like wild-type Nox4, chimera Nox2/4 ROS generating activity was constitutively active and was independent of regulatory subunits or PMA stimulation. In contrast, chimera Nox4/2, like wild-type Nox2, displayed activity only upon coexpression of subunits and stimulation with PMA. Therefore, the Nox2 DH domain contains the determinants that are the target of regulatory subunit binding and regulation, while the structural features necessary for constitutive activity reside in the Nox4 DH domain.

Electron Transferase Activity of Nox DH Domains. Experiments conducted with chimeric proteins indicated that the Nox4 DH domain is necessary to observe the constitutive activity of Nox4. To determine whether this domain was sufficient to exhibit spontaneous electron transferase activity, the Nox4 DH domain was expressed and purified as an MBP fusion protein and electron transferase activity toward several artificial electron acceptors was measured. For comparison, Nox1, Nox2, and Nox5 DH domains were also expressed and purified. MBP−Nox DH domain fusion proteins corresponded in size to their predicted molecular masses on SDS−PAGE (Figure 3A) and were recognized on Western blots using an anti-MBP antibody (Figure 3B). The MBP-fused forms of the Nox DH domains were used in this study because of the poor solubility of the DH domains when the MBP tag was omitted or cleaved. Figure 4 shows the NADPH-dependent electron transferase activity of each isolated Nox DH domain, assayed using cytochrome *c*, cytochrome b_5, ferricyanide, DCIP, INT, or NBT as an electron acceptor. The MBP−Nox4 DH domain fusion protein showed significant NADPH-dependent electron transferase activity toward both one-electron acceptors and two-electron accepting dyes, and turnover numbers varied somewhat according to the electron acceptor employed, with ferricyanide being the best electron accepting substrate

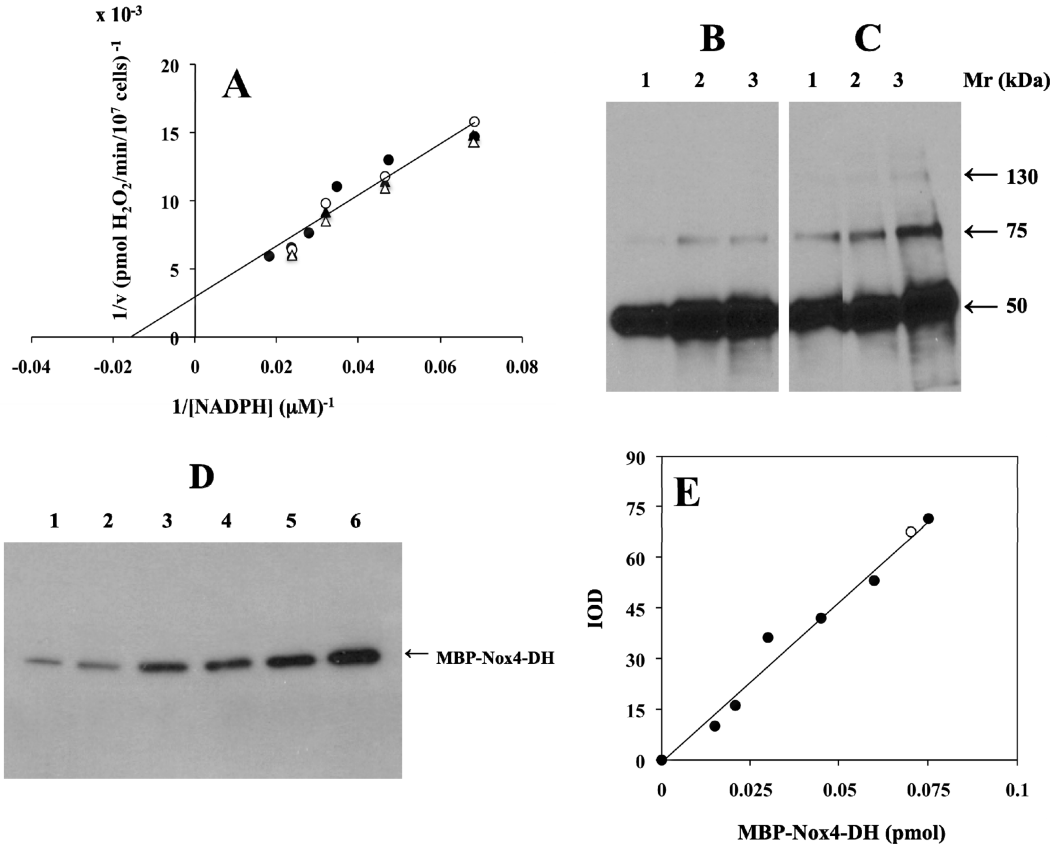

FIGURE 1: Nox4-dependent hydrogen peroxide generation in HEK293 cell lysates. (A) Hydrogen peroxide production by cell lysates was measured in the presence of various concentrations of FAD: 20 (●), 25 (○), 50 (▲), and 75 μM (△). The rate was determined at various concentrations of NADPH, and a double-reciprocal plot of initial velocity vs NADPH concentration was used to estimate K_m and V_{max} values at each concentration of FAD. The reaction velocity (v) due to the overexpressed Nox4 was determined by subtracting the activity of the empty vector-transfected cells as in Table 1. The data are representative of three separate experiments. (B and C) Expression of Nox4 protein in HEK293 cells. Extracts (0.85 mg of protein) from both empty vector-transfected cells (B) and Nox4 cDNA-transfected cells (C) were subjected to immunoprecipitation using an antibody to Nox4. Lanes 1−3 contained 3, 6, and 10 μL, respectively, of SDS sample buffer containing proteins immunoprecipitated with protein A-agarose beads Fast Flow [50% (v/v)]. SDS−PAGE (7.5%) followed by Western blotting was used to visualize Nox4 protein. The 50 kDa band indicated by an arrow is the IgG heavy chain. (D) Immunoblot of the purified MBP−Nox4 DH domain fusion protein. In lanes 1−6, 0.012−0.075 pmol of purified MBP−Nox4 DH domain fusion protein was applied. (E) The standard curve was obtained by plotting the amount of MBP−Nox4 DH domain fusion protein loaded vs the IOD (integral optical density) of the band visualized in panel D. Filled circles show data for the standard MBP−Nox4 DH domain fusion protein, while the empty circle indicates the IOD and determined Nox4 content of the 75 kDa holo-Nox4 band in lane 3 in panel C. The experiment shown is representative of three.

(470 min^{-1}), followed by DCIP (180 min^{-1}), cytochrome c (160 min^{-1}), INT (95 min^{-1}), cytochrome b_5 (75 min^{-1}), and NBT (65 min^{-1}, the least active). The high rate seen with ferricyanide is typical of many flavoprotein dehydrogenases, presumably due to the favorable access of this small chelated iron acceptor to the FAD. In contrast to the cytochrome c reductase activity of the intact Nox2 system, Nox4 DH domain reduction of this substrate was largely unaffected by added SOD (data not shown) and is therefore due to a direct electron transfer from the enzyme FAD rather than a superoxide-mediated reaction. In contrast, Nox1, Nox2, and Nox5 DH domains exhibited only very low NADPH-dependent electron transferase rates (<1 min^{-1}), regardless of the electron acceptor (Figure 4), and no activity was observed using NADH as the electron donor (data not shown). Previously, we reported that the presence of activating subunits stimulated diaphorase activity of the Nox2 DH domain (*4*). The turnover, however, was still very low (<10 min^{-1}) compared with that seen with Nox4. MBP alone showed no activity, and MBP−Nox4 DH domain activity was inhibited by 70% or more with DPI for all electron acceptors. Little or no Nox4 DH domain-dependent activity was observed in the absence of added FAD, indicating loss of FAD during the purification. For all electron acceptors, Nox4 DH domain-dependent activities were very low using NADH rather than NADPH as an electron donor

FAD and NADPH Concentration-Dependent Electron Transferase Activities of Nox2 DH and Nox4 DH Domains. Cytochrome c reduction provided a convenient assay with which to determine kinetic parameters of the Nox4 DH domain. The EC_{50} of the FAD for activation of Nox4 DH domain-dependent cytochrome c reduction was 65 ± 10 μM [Figure 5A (●)]. In contrast, FAD failed to stimulate the activity of the Nox2 DH domain up to 0.3 mM [Figure 5A (○)]. The K_m for NADPH for the Nox4 DH domain was 20 ± 5 μM (Figure 5B). In addition, DPI inhibited NADPH-specific cytochrome c reductase activity of the Nox4 DH domain in a concentration-dependent manner, but rotenone, used as a negative control, did not (Figure 5C).

DISCUSSION

The functional role of the DH domain of Nox enzymes, aside from binding FAD and NADPH, is to catalyze the transfer of reducing equivalents from NADPH through FAD to the heme iron of flavocytochrome b_{558}. Nox1−4 form a heterodimer with the $p22^{phox}$ subunit that is essential for their catalytic activity and structural stability. Unlike Nox4, Nox1−3 require additional

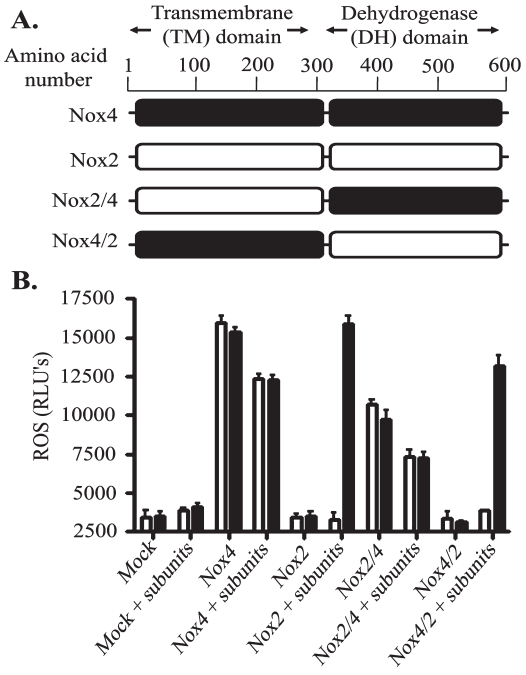

FIGURE 2: ROS generation of Nox4/2 and Nox2/4 chimeric proteins and regulation by phox regulatory subunits. (A) Schematic model of Nox2/4 and Nox4/2 chimeric proteins showing Nox2 TM/Nox4 DH and Nox4 TM/Nox2 DH, respectively. (B) cDNA encoding Nox4 (wild type), Nox2 (wild type), Nox2/4, Nox4/2, or empty vector alone (mock) was transfected with or without coexpression of cytosolic subunit proteins ($p67^{phox}$, $p47^{phox}$, and Rac1G12V) in HEK293 cells. ROS production was measured by Luminol chemiluminescence in the oxidase assay buffer in the absence (white bars) and presence (black bars) of PMA at 37 °C. Three separate transfection experiments were conducted, and the activity is shown as mean relative light units (RLUs) ± the standard deviation ($n = 3$).

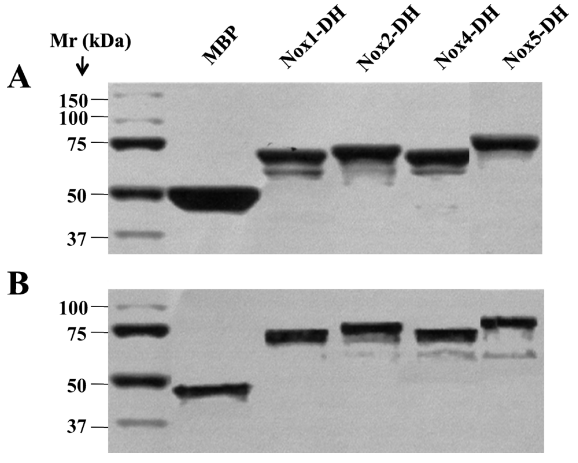

FIGURE 3: Isolated dehydrogenase domains of Nox homologues. (A) MBP fusion forms of Nox1 DH, Nox2 DH, Nox4 DH, and Nox5 DH domain purified proteins (~4.5 μg) were loaded onto a 10% (w/v) SDS−PAGE gel and stained with Coomassie brilliant blue. (B) Nox-DH proteins (~1.2 μg) were subjected to 10% SDS−PAGE, followed by immunoblotting using an anti-MBP antibody.

regulatory subunits while Nox5, Duox1, and Duox2 are activated by their calcium-binding regulatory domains. The constitutive activity of Nox4 is independent of known regulatory subunits or domains, and features of its structure are therefore expected to resemble the activated state that is achieved in the other Nox or Duox proteins in response to regulatory protein−protein interactions. Our previous studies (*4*, *5*) of Nox2 DH domain−$p67^{phox}$ interaction and indirect evidence from X-linked CGD mutations (*49*, *50*) indicated that binding of $p67^{phox}$ to Nox2 stimulates the flow of electrons from NADPH to FAD (*51*, *52*). Our studies were based on the ability of phagocyte oxidase regulatory subunits to stimulate a low rate of NADPH-dependent dye reduction activity by the Nox2 DH domain. In support of this interpretation, our Nox4/2 chimera (see Figure 2) is inactive in the basal state but is activated to near wild-type activity by subunits with PMA. In contrast, like wild-type Nox4, the reverse chimera Nox2/4 shows constitutive activity that is unaffected by regulatory subunit cotransfection or PMA. Consistent with these data, a recent study reported constitutive activity by a Nox1/4 chimera (Nox1 TM and Nox4 DH) that was independent of the Nox1 regulatory subunits NOXO1 and NOXA1 (*40*). In contrast, a study published as this work was being completed (*53*) reported that a Nox2/4 chimera was inactive. The reason for this discrepancy may be that the chimera junctions (i.e., the amino acid boundary where the sequence changes from the Nox2 TM domain to the Nox4 DH domain) are not the same between our Nox2/4 chimera (which ends the Nox2 TM domain at amino acid 284 and begins the Nox4 DH domain at amino acid 298) and the Nox2/4 chimera reported in the recent study (*53*) (which ends the Nox2 TM domain at amino acid 290 and begins the Nox4 DH domain at amino acid 304). We have made several Nox2/4 chimeras with slightly different junctions, and we find that small differences in position at which the DH domain begins can drastically decrease or eliminate activity (data not shown). Thus, both our study and the earlier studies of the Nox1/4 chimera support the idea that the DH domain rather than the TM domain is a major determinant of the overall activity and is the target for regulation by activating subunits.

To further explore this hypothesis and determine whether the DH domain is not only necessary but also sufficient for determining the overall activity, we expressed the DH domains from Nox1, Nox2, Nox4, and Nox5 and investigated their intrinsic activity toward nonphysiological dyes or proteins. The steps in electron transfer that occur within the Nox DH domain are an initial two-electron transfer from NADPH to FAD with subsequent one-electron transfers from the reduced and semiquinone flavin to heme. In these experiments, the heme-containing TM domain is replaced with exogenous hemoproteins (cytochrome *c* and cytochrome b_5 lacking the hydrophobic membrane-anchoring domain), the small iron-containing ferricyanide, or various dyes. The midpoint redox potentials of these acceptors ranged from 20 mV for soluble cytochrome b_5 to 360 mV for ferricyanide, all significantly higher than the redox potential of the FAD of known flavoprotein dehydrogenases (*54*−*56*). No correlation between the reduction rate and redox potential of the electron acceptor was seen, indicating that other factors (e.g., the reduction of the FAD, steric access of the electron acceptor to the FAD, etc.) are more important in the determination of the overall rate. While the DH domains from Nox1, Nox2, and Nox5 exhibited very low activity (< 1 min^{-1}), the Nox4 DH domain showed significant rates of electron transfer (65−470 min^{-1} depending on the electron acceptor), and these activities were inhibited by DPI. The most rapid rate of reduction was seen with ferricyanide as an electron acceptor, a phenomenon that has been observed with many flavoprotein dehydrogenases and which is often taken to be a measure of the rate of reduction of the FAD (*34*, *57*, *58*). The rapid reduction may be permitted due to the small size of this acceptor (allowing close approach to the reduced FAD), the very positive redox potential, and/or additional

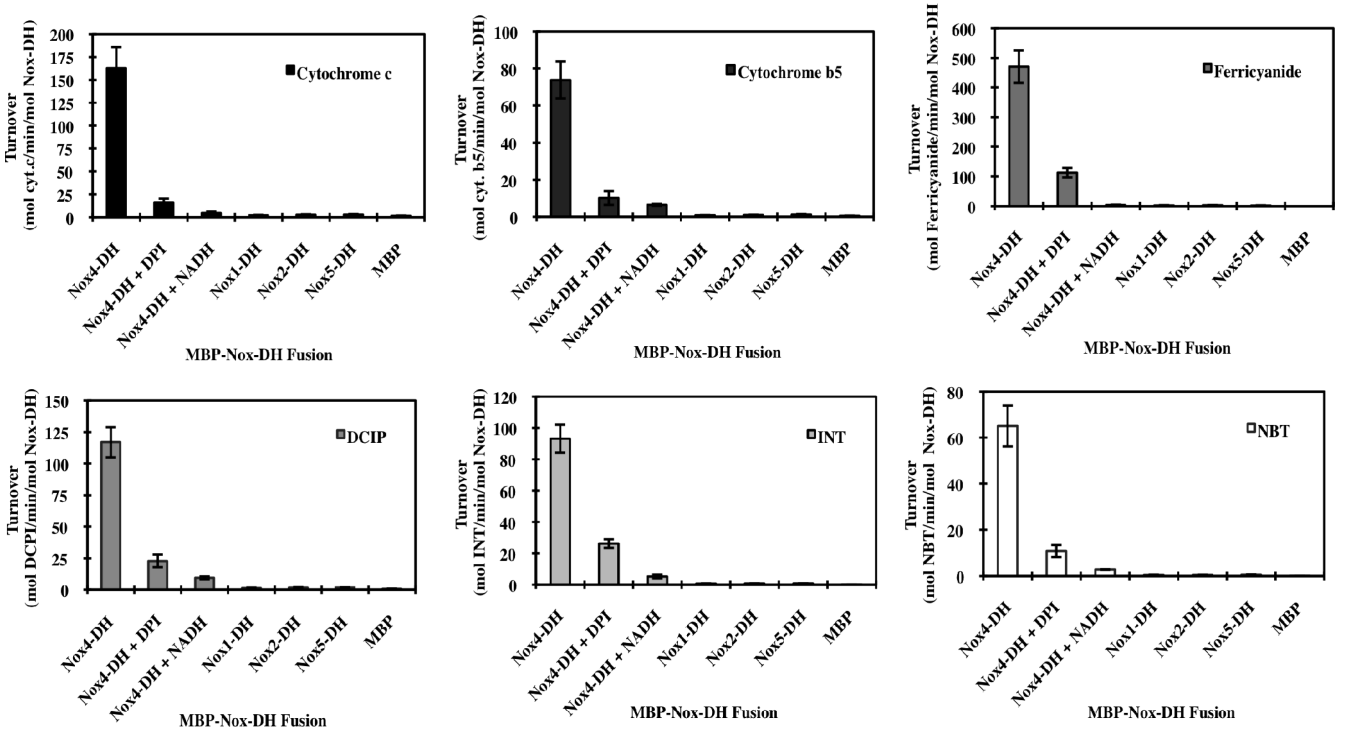

FIGURE 4: Pyridine nucleotide-dependent electron transferase activities of Nox1 DH, Nox2 DH, Nox4 DH, and Nox5 DH domains. Isoforms of the MBP-fused Nox DH domain (~25 μg) and MBP alone were assayed for cytochrome *c*, cytochrome b_5, ferricyanide, DCIP, INT, and NBT reductase activities. The assay was initiated via addition of 0.25 mM NADPH or 0.25 mM NADH to 1 mL of 25 mM Hepes (pH 7.3) containing 0.12 M NaCl, 3 mM KCl, 1 mM $MgCl_2$, protease inhibitor cocktail (1 μg), 0.25 mM FAD, and 80 μM electron acceptor. NADPH was used in all the experiments, except where NADH is indicated in the third bar of each figure. The NADPH-dependent reductive reaction of Nox4-DH was conducted without (first column) or with (second column) 20 μM DPI preincubated at 36 °C for 30 s. Each reductive activity indicates the turnover number mean of three independent assays, with the error bars showing the standard deviation.

unknown factors. For NADPH-dependent cytochrome *c* reductase activity, which is often used as a readout for superoxide generation, there was no significant decrease in activity in the presence of SOD, indicating that the DH domain of Nox4 generates little if any superoxide. Rather, the reduction of this hemoprotein must occur directly from reduced forms of the enzyme-bound FAD. Therefore, in this setting, cytochrome *c* provides a model for the endogenous NADPH-to-FAD-to-heme reduction that occurs in the holoenzyme. In previous studies, we were able to show an increase in the rate of NADPH-dependent reduction of artificial electron acceptors catalyzed by the Nox2 DH domain as a result of addition of the Rac−$p67^{phox}$ complex, pointing to the DH domain as the locus of regulation in Nox2 (*4*).

A consistent picture showing that properties of the DH domain determine the overall rate of electron transfer through the Nox catalytic units during the generation of reactive oxygen species emerges from this study and earlier studies. This is in accord with earlier studies (*5*) which pointed to the transfer of hydride from NADPH to FAD to form $FADH_2$ as the rate-determining step in Nox2, a step that is regulated by the activation domain of $p67^{phox}$. In addition, during turnover of activated Nox2, FAD is maintained in a mostly oxidized (~70%) form, while heme remains almost entirely oxidized, again indicating that in the activated enzyme, FAD reduction is the rate-limiting step. While this type of experiment is not feasible with Nox4 due to low expression levels, these studies are consistent with this model for Nox4 activity. The correspondence in turnover number of intact Nox4 during the NADPH-dependent formation of hydrogen peroxide (200 min^{-1}) and NADPH-dependent electron transfer rates to artificial substrates (65−470 min^{-1}) strongly suggests that FAD reduction represents the rate-determining step in holo-Nox4.

As a reflection of earlier uncertainties about the pyridine nucleotide specificity of novel Nox enzymes, the class of enzymes has previously been termed NAD(P)H oxidases (note parentheses). Sumimoto and colleagues (*21*) reported that the specificity of Nox4 was for NADH, while Serrander and colleagues reported specificity for NADPH (*41*). Using our lysed cell system, this study shows a clear specificity of Nox4 for NADPH, and the K_m of 55 ± 10 μM is nearly the same as that reported for the phagocyte oxidase (Nox2) cell-free system (*43*). The expressed and purified Nox4 DH domain also shows a nearly complete preference for NADPH over NADH. Therefore, we propose that for Nox4, the terminology NAD(P)H oxidase be abandoned in favor of NADPH oxidase. We suggest that the somewhat lower K_m of the Nox4 DH domain for NADPH of 20 ± 5 μM (Figure 5B) reflects a somewhat less efficient transfer of electrons from FAD to the heme of cytochrome *c* compared with the native heme A, which would result in a lower K_m based solely on the combination of kinetic constants that govern K_m [i.e., $(k_2 + k_{-1})/k_1$] that yield a higher K_m value when k_2 is larger. Comparison of the activity in intact cells versus cell lysates also indicated that most of the Nox4 activity was recovered in broken cell preparations. In addition, the activity appears to be relatively stable to storage at 4 °C (data not shown).

While appreciable, the turnover number for Nox4 in the transfected cell system is considerably lower than that of the phagocyte enzyme, which has been reported to be > 5000 min^{-1}. It is possible that the lower turnover is an artifact of the overexpression system and that only a fraction of expressed Nox4 is actually active. While this cannot be rigorously ruled out at present, the lower rate is also consistent with respective biological functions, with Nox2 being optimized for high activity to generate bactericidal

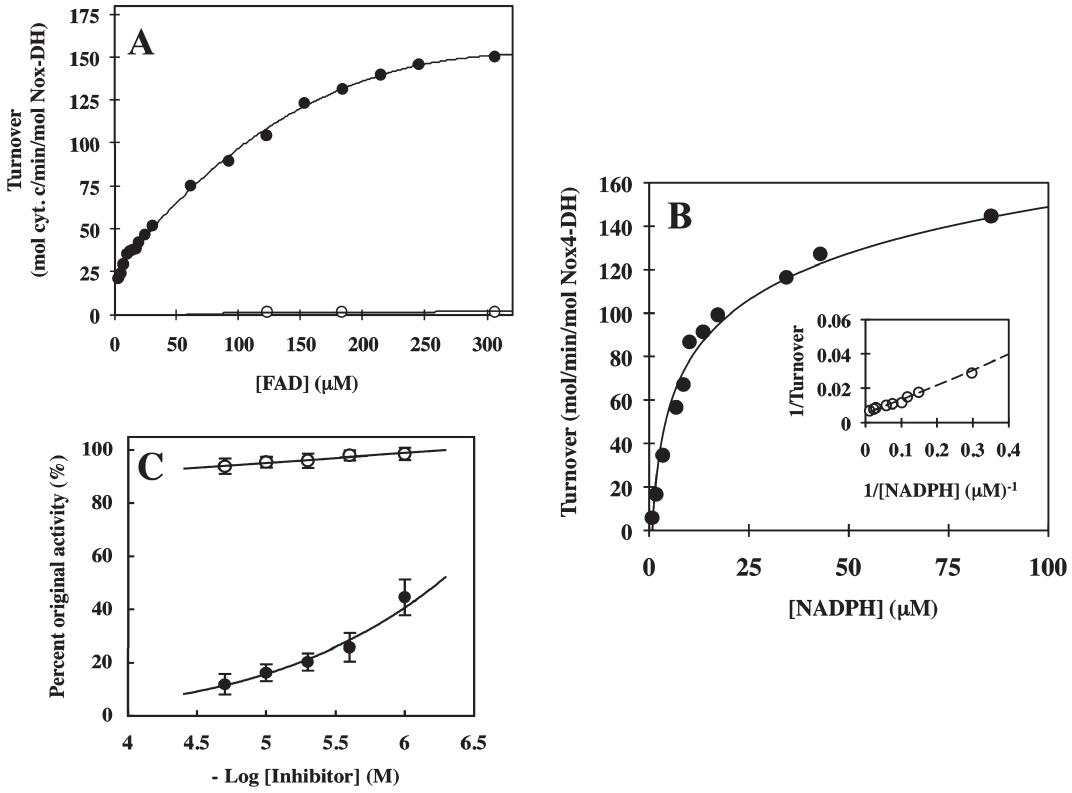

FIGURE 5: Kinetic properties of the Nox4 DH domain. (A) The MBP-tagged Nox DH domain [Nox4 DH domain (●) and Nox2 DH domain (○), 22 μg each] was preincubated with 1.2−300 μM FAD in assay buffer containing 80 μM cytochrome *c* at 20 °C for 15 min. NADPH-dependent cytochrome *c* reduction, followed spectrophotometrically at 550 nm, was initiated via addition of 0.25 mM NADPH at 36 °C. Results shown are representative of four experiments. (B) Cytochrome *c* reduction was measured as a function of NADPH concentration (0.66−85 μM). The inset shows a double-reciprocal plot of initial velocity vs substrate concentration. (C) The MBP−Nox4 DH domain fusion protein (20 μg) was incubated with 0.3 mM FAD at 20 °C for 15 min and then assayed for NADPH-dependent cytochrome *c* reduction in the presence of either DPI (●) or rotenone (○). Results are expressed as a percentage of the uninhibited cytochrome *c* reduction rate determined in a separate assay. Error bars indicate the standard error of three determinations.

quantities of ROS and Nox4 requiring lower activity to generate signaling levels of H_2O_2. Alternatively, the rate observed may represent a low basal rate that can be further stimulated by unknown regulatory factors that are not present in the HEK293 cells. For example, in a recent study, the $p22^{phox}$-binding protein Poldip2 produced a modest stimulation of Nox4 activity in rat smooth muscle cells, although it not clear whether this was due to activation or protein stabilization (*59*).

In summary, the implication of this study is the Nox4 DH domain exists in a conformation that allows the spontaneous transfer of electrons from NADPH to FAD, and this property of the DH domain explains the constitutive activity of Nox4.

ACKNOWLEDGMENT

We express appreciation to Dr. Toshitsugu Yubisui (Department of Biochemistry, Okayama University of Science, Okayama, Japan) for the gift of soluble cytochrome b_5 protein. We also thank Dr. Yerun Zhu (Department of Pathology, Emory University Medical School) for technical suggestions on the fluorophotometric ROS assay.

REFERENCES

1. Segal, A. W., West, I., Wientjes, F., Nugent, J. H., Chavan, A. J., Haley, B., Garcia, R. C., Rosen, H., and Scrace, G. (1992) Cytochrome b-245 is a flavocytochrome containing FAD and the NADPH-binding site of the microbicidal oxidase of phagocytes. *Biochem. J. 284* (Part 3), 781–788.
2. Sumimoto, H., Sakamoto, N., Nozaki, M., Sakaki, Y., Takeshige, K., and Minakami, S. (1992) Cytochrome b558, a component of the phagocyte NADPH oxidase, is a flavoprotein. *Biochem. Biophys. Res. Commun. 186*, 1368–1375.
3. Rotrosen, D., Yeung, C. L., Leto, T. L., Malech, H. L., and Kwong, C. H. (1992) Cytochrome b558: The flavin-binding component of the phagocyte NADPH oxidase. *Science 256*, 1459–1462.
4. Nisimoto, Y., Ogawa, H., Miyano, K., and Tamura, M. (2004) Activation of the flavoprotein domain of gp91phox upon interaction with N-terminal p67phox (1−210) and the Rac complex. *Biochemistry 43*, 9567–9575.
5. Nisimoto, Y., Motalebi, S., Han, C. H., and Lambeth, J. D. (1999) The p67(phox) activation domain regulates electron flow from NADPH to flavin in flavocytochrome b(558). *J. Biol. Chem. 274*, 22999–23005.
6. Han, C. H., Freeman, J. L., Lee, T., Motalebi, S. A., and Lambeth, J. D. (1998) Regulation of the neutrophil respiratory burst oxidase. Identification of an activation domain in p67(phox). *J. Biol. Chem. 273*, 16663–16668.
7. Banfi, B., Maturana, A., Jaconi, S., Arnaudeau, S., Laforge, T., Sinha, B., Ligeti, E., Demaurex, N., and Krause, K. H. (2000) A mammalian H^+ channel generated through alternative splicing of the NADPH oxidase homolog NOH-1. *Science 287*, 138–142.
8. Laurent, E., McCoy, J. W., III, Macina, R. A., Liu, W., Cheng, G., Robine, S., Papkoff, J., and Lambeth, J. D. (2008) Nox1 is over-expressed in human colon cancers and correlates with activating mutations in K-Ras. *Int. J. Cancer 123*, 100–107.
9. Kikuchi, H., Hikage, M., Miyashita, H., and Fukumoto, M. (2000) NADPH oxidase subunit, gp91(phox) homologue, preferentially expressed in human colon epithelial cells. *Gene 254*, 237–243.
10. Lassegue, B., Sorescu, D., Szocs, K., Yin, Q., Akers, M., Zhang, Y., Grant, S. L., Lambeth, J. D., and Griendling, K. K. (2001) Novel gp91(phox) homologues in vascular smooth muscle cells: nox1 mediates angiotensin II-induced superoxide formation and redox-sensitive signaling pathways. *Circ. Res. 88*, 888–894.
11. Wingler, K., Wunsch, S., Kreutz, R., Rothermund, L., Paul, M., and Schmidt, H. H. (2001) Upregulation of the vascular NAD(P)H-oxidase isoforms Nox1 and Nox4 by the renin-angiotensin

system in vitro and in vivo. *Free Radical Biol. Med. 31*, 1456–1464.
12. Takeya, R., Ueno, N., Kami, K., Taura, M., Kohjima, M., Izaki, T., Nunoi, H., and Sumimoto, H. (2003) Novel human homologues of p47phox and p67phox participate in activation of superoxide-producing NADPH oxidases. *J. Biol. Chem. 278*, 25234–25246.
13. Banfi, B., Clark, R. A., Steger, K., and Krause, K. H. (2003) Two novel proteins activate superoxide generation by the NADPH oxidase NOX1. *J. Biol. Chem. 278*, 3510–3513.
14. Geiszt, M., Lekstrom, K., Witta, J., and Leto, T. L. (2003) Proteins homologous to p47phox and p67phox support superoxide production by NAD(P)H oxidase 1 in colon epithelial cells. *J. Biol. Chem. 278*, 20006–20012.
15. Cheng, G., Diebold, B. A., Hughes, Y., and Lambeth, J. D. (2006) Nox1-dependent reactive oxygen generation is regulated by Rac1. *J. Biol. Chem. 281*, 17718–17726.
16. Banfi, B., Malgrange, B., Knisz, J., Steger, K., Dubois-Dauphin, M., and Krause, K. H. (2004) NOX3, a superoxide-generating NADPH oxidase of the inner ear. *J. Biol. Chem. 279*, 46065–46072.
17. Cheng, G., Ritsick, D., and Lambeth, J. D. (2004) Nox3 regulation by NOXO1, p47phox, and p67phox. *J. Biol. Chem. 279*, 34250–34255.
18. Ueno, N., Takeya, R., Miyano, K., Kikuchi, H., and Sumimoto, H. (2005) The NADPH oxidase Nox3 constitutively produces superoxide in a p22phox-dependent manner: its regulation by oxidase organizers and activators. *J. Biol. Chem. 280*, 23328–23339.
19. Ueyama, T., Geiszt, M., and Leto, T. L. (2006) Involvement of Rac1 in activation of multicomponent Nox1- and Nox3-based NADPH oxidases. *Mol. Cell. Biol. 26*, 2160–2174.
20. Geiszt, M., Kopp, J. B., Varnai, P., and Leto, T. L. (2000) Identification of renox, an NAD(P)H oxidase in kidney. *Proc. Natl. Acad. Sci. U.S.A. 97*, 8010–8014.
21. Shiose, A., Kuroda, J., Tsuruya, K., Hirai, M., Hirakata, H., Naito, S., Hattori, M., Sakaki, Y., and Sumimoto, H. (2001) A novel superoxide-producing NAD(P)H oxidase in kidney. *J. Biol. Chem. 276*, 1417–1423.
22. Kawahara, T., Ritsick, D., Cheng, G., and Lambeth, J. D. (2005) Point mutations in the proline-rich region of p22phox are dominant inhibitors of Nox1- and Nox2-dependent reactive oxygen generation. *J. Biol. Chem. 280*, 31859–31869.
23. Ambasta, R. K., Kumar, P., Griendling, K. K., Schmidt, H. H., Busse, R., and Brandes, R. P. (2004) Direct interaction of the novel Nox proteins with p22phox is required for the formation of a functionally active NADPH oxidase. *J. Biol. Chem. 279*, 45935–45941.
24. Parkos, C. A., Dinauer, M. C., Walker, L. E., Allen, R. A., Jesaitis, A. J., and Orkin, S. H. (1988) Primary structure and unique expression of the 22-kilodalton light chain of human neutrophil cytochrome b. *Proc. Natl. Acad. Sci. U.S.A. 85*, 3319–3323.
25. Martyn, K. D., Frederick, L. M., von Loehneysen, K., Dinauer, M. C., and Knaus, U. G. (2006) Functional analysis of Nox4 reveals unique characteristics compared to other NADPH oxidases. *Cell. Signalling 18*, 69–82.
26. Banfi, B., Molnar, G., Maturana, A., Steger, K., Hegedus, B., Demaurex, N., and Krause, K. H. (2001) A Ca^{2+}-activated NADPH oxidase in testis, spleen, and lymph nodes. *J. Biol. Chem. 276*, 37594–37601.
27. Banfi, B., Tirone, F., Durussel, I., Knisz, J., Moskwa, P., Molnar, G. Z., Krause, K. H., and Cox, J. A. (2004) Mechanism of Ca^{2+} activation of the NADPH oxidase 5 (NOX5). *J. Biol. Chem. 279*, 18583–18591.
28. Dupuy, C., Ohayon, R., Valent, A., Noel-Hudson, M. S., Deme, D., and Virion, A. (1999) Purification of a novel flavoprotein involved in the thyroid NADPH oxidase. Cloning of the porcine and human cdnas. *J. Biol. Chem. 274*, 37265–37269.
29. Diebold, B. A., and Bokoch, G. M. (2001) Molecular basis for Rac2 regulation of phagocyte NADPH oxidase. *Nat. Immunol. 2*, 211–215.
30. Nisimoto, Y., Tsubouchi, R., Diebold, B. A., Qiao, S., Ogawa, H., Ohara, T., and Tamura, M. (2008) Activation of NADPH oxidase 1 in tumour colon epithelial cells. *Biochem. J. 415*, 57–65.
31. Major, M. L., Lepe, R., and Costa, R. H. (2004) Forkhead box M1B transcriptional activity requires binding of Cdk-cyclin complexes for phosphorylation-dependent recruitment of p300/CBP coactivators. *Mol. Cell. Biol. 24*, 2649–2661.
32. Lutter, R., van Schaik, M. L., van Zwieten, R., Wever, R., Roos, D., and Hamers, M. N. (1985) Purification and partial characterization of the b-type cytochrome from human polymorphonuclear leukocytes. *J. Biol. Chem. 260*, 2237–2244.
33. Shiraki, K., Kudou, M., Fujiwara, S., Imanaka, T., and Takagi, M. (2002) Biophysical effect of amino acids on the prevention of protein aggregation. *J. Biochem. 132*, 591–595.
34. Vermilion, J. L., Ballou, D. P., Massey, V., and Coon, M. J. (1981) Separate roles for FMN and FAD in catalysis by liver microsomal NADPH-cytochrome P-450 reductase. *J. Biol. Chem. 256*, 266–277.
35. Kimura, S., Nishida, H., and Iyanagi, T. (2001) Effects of flavin-binding motif amino acid mutations in the NADH-cytochrome b5 reductase catalytic domain on protein stability and catalysis. *J. Biochem. 130*, 481–490.
36. Schellenberg, K. A., and Hellerman, L. (1958) Oxidation of reduced diphosphopyridine nucleotide. *J. Biol. Chem. 231*, 547–556.
37. Norager, S., Arent, S., Bjornberg, O., Ottosen, M., Lo Leggio, L., Jensen, K. F., and Larsen, S. (2003) *Lactococcus lactis* dihydroorotate dehydrogenase A mutants reveal important facets of the enzymatic function. *J. Biol. Chem. 278*, 28812–28822.
38. Pessach, I., Leto, T. L., Malech, H. L., and Levy, R. (2001) Essential requirement of cytosolic phospholipase A(2) for stimulation of NADPH oxidase-associated diaphorase activity in granulocyte-like cells. *J. Biol. Chem. 276*, 33495–33503.
39. Mitchell, J. A., Kohlhaas, K. L., Matsumoto, T., Pollock, J. S., Forstermann, U., Warner, T. D., Schmidt, H. H., and Murad, F. (1992) Induction of NADPH-dependent diaphorase and nitric oxide synthase activity in aortic smooth muscle and cultured macrophages. *Mol. Pharmacol. 41*, 1163–1168.
40. Helmcke, I., Heumuller, S., Tikkanen, R., Schroder, K., and Brandes, R. P. (2009) Identification of structural elements in Nox1 and Nox4 controlling localization and activity. *Antioxid. Redox Signaling 11*, 1279–1287.
41. Serrander, L., Cartier, L., Bedard, K., Banfi, B., Lardy, B., Plastre, O., Sienkiewicz, A., Forro, L., Schlegel, W., and Krause, K. H. (2007) NOX4 activity is determined by mRNA levels and reveals a unique pattern of ROS generation. *Biochem. J. 406*, 105–114.
42. Chen, K., Kirber, M. T., Xiao, H., Yang, Y., and Keaney, J. F., Jr. (2008) Regulation of ROS signal transduction by NADPH oxidase 4 localization. *J. Cell Biol. 181*, 1129–1139.
43. Bromberg, Y., and Pick, E. (1984) Unsaturated fatty acids stimulate NADPH-dependent superoxide production by cell-free system in macrophages. *Cell. Immunol. 88*, 213–221.
44. Bellavite, P., Cross, A. R., Serra, M. C., Davoli, A., Jones, O. T., and Rossi, F. (1983) The cytochrome b and flavin content and properties of the O_2^--forming NADPH oxidase solubilized from activated neutrophils. *Biochim. Biophys. Acta 746*, 40–47.
45. Cross, A. R., Parkinson, J. F., and Jones, O. T. (1984) The superoxide-generating oxidase of leucocytes. NADPH-dependent reduction of flavin and cytochrome b in solubilized preparations. *Biochem. J. 223*, 337–344.
46. Yoshida, L. S., Saruta, F., Yoshikawa, K., Tatsuzawa, O., and Tsunawaki, S. (1998) Mutation at histidine 338 of gp91(phox) depletes FAD and affects expression of cytochrome b558 of the human NADPH oxidase. *J. Biol. Chem. 273*, 27879–27886.
47. Lambeth, J. D. (2004) NOX enzymes and the biology of reactive oxygen. *Nat. Rev. Immunol. 4*, 181–189.
48. Vignais, P. V. (2002) The superoxide-generating NADPH oxidase: Structural aspects and activation mechanism. *Cell. Mol. Life Sci. 59*, 1428–1459.
49. Leusen, J. H., de Boer, M., Bolscher, B. G., Hilarius, P. M., Weening, R. S., Ochs, H. D., Roos, D., and Verhoeven, A. J. (1994) A point mutation in gp91-phox of cytochrome b558 of the human NADPH oxidase leading to defective translocation of the cytosolic proteins p47-phox and p67-phox. *J. Clin. Invest. 93*, 2120–2126.
50. Li, X. J., Fieschi, F., Paclet, M. H., Grunwald, D., Campion, Y., Gaudin, P., Morel, F., and Stasia, M. J. (2007) Leu505 of Nox2 is crucial for optimal p67phox-dependent activation of the flavocytochrome b558 during phagocytic NADPH oxidase assembly. *J. Leukocyte Biol. 81*, 238–249.
51. Cross, A. R., and Curnutte, J. T. (1995) The cytosolic activating factors p47phox and p67phox have distinct roles in the regulation of electron flow in NADPH oxidase. *J. Biol. Chem. 270*, 6543–6548.
52. Cross, A. R., Yarchover, J. L., and Curnutte, J. T. (1994) The superoxide-generating system of human neutrophils possesses a novel diaphorase activity. Evidence for distinct regulation of electron flow within NADPH oxidase by p67-phox and p47-phox. *J. Biol. Chem. 269*, 21448–21454.
53. von Lohneysen, K., Noack, D., Wood, M. R., Friedman, J. S., and Knaus, U. G. (2009) Structural Insights into Nox4 and Nox2: Motifs Involved in Function and Cellular Localization. *Mol. Cell. Biol. 30*, 961–975.
54. Zhang, H., Whitelegge, J. P., and Cramer, W. A. (2001) Ferredoxin: $NADP^+$ oxidoreductase is a subunit of the chloroplast cytochrome b6f complex. *J. Biol. Chem. 276*, 38159–38165.
55. Iyanagi, T., and Mason, H. S. (1973) Some properties of hepatic reduced nicotinamide adenine dinucleotide phosphate-cytochrome c reductase. *Biochemistry 12*, 2297–2308.

56. Roman, L. J., McLain, J., and Masters, B. S. (2003) Chimeric enzymes of cytochrome P450 oxidoreductase and neuronal nitric-oxide synthase reductase domain reveal structural and functional differences. *J. Biol. Chem. 278*, 25700–25707.
57. Takesue, S., and Omura, T. (1970) Solubilization of NADH-cytochrome b5 reductase from liver microsomes by lysosomal digestion. *J. Biochem. 67*, 259–266.
58. Olson, S. T., and Massey, V. (1979) Purification and properties of the flavoenzyme D-lactate dehydrogenase from *Megasphaera elsdenii*. *Biochemistry 18*, 4714–4724.
59. Lyle, A. N., Deshpande, N. N., Taniyama, Y., Seidel-Rogol, B., Pounkova, L., Du, P., Papaharalambus, C., Lassegue, B., and Griendling, K. K. (2009) Poldip2, a novel regulator of Nox4 and cytoskeletal integrity in vascular smooth muscle cells. *Circ. Res. 105*, 249–259.